I gratefully acknowledge the support of the Laidlaw Foundation, whose financial assistance has been a cornerstone in bringing this innovative project to fruition. I would also like to extend my gratitude to my research supervisor, Amy Bilton from the Mechanical and Industrial Engineering Department at The University of Toronto, for her invaluable guidance, expertise, and persistent encouragement throughout this research journey.

-Vishweswar Eswaran
BASc Electrical Engineering (2021-25), UofT
Laidlaw Scholar 2023-24

Wearable system for applied force sensing during telemedicine operations

Vishweswar Eswaran, Amy Bilton

Abstract— **This report outlines the development of a telemedicine device utilizing telepresence technologies, focusing on tactile modality in cardiopulmonary resuscitation. The highlighted design is a modular wearable sensor array integrated into a glove, enabling the remote monitoring of palm contact forces during medical interventions. The device aims to facilitate remote cardiopulmonary resuscitation and other physical interventions, especially in emergency scenarios where immediate transportation is not viable. The modular design allows for customization and easy integration with existing telemedicine infrastructure. This preliminary prototype represents the initial phase of a project with potential, including further enhancements in circuit fidelity, faster data processing, and the development of a haptic rendering glove for a more immersive remote healthcare experience. Future iterations of this technology may revolutionize remote medical interventions, making healthcare more accessible and effective.**

I. INTRODUCTION

Telemedicine plays a crucial role in enabling medically remote areas to have access to healthcare services. It helps in overcoming socio economic barriers to treatment, reduces workload on the healthcare system, and improves patient-therapist communication. Telepresence technologies (a pivotal element of telemedicine) can facilitate more effective and safer healthcare service delivery [1]. Telepresence can be achieved through multimedia sensory feedback that involves haptic/tactile, sound, vision or olfactory. Tactile modality, particularly, has found wider use in the field of medicine and minimally invasive robotic surgery. Integrating tactile feedback in robotic surgery would expand the role of robotics in clinical tests and examinations requiring palpation [2].

II. TACTILE MODALITY

Tactile modality of communication in telemedicine enables the conveyance of the physical sensations of touch from one location to another. The entities involved in the two-way communication process are:

1. The patient who requires a physical intervention for diagnostic or treatment purposes.
2. The end effector (a human or robotic entity) that intervenes the patient physically for diagnostic or treatment purposes.
3. The remote manipulator, typically a healthcare professional, intervening the patient from a distance via the end effector.

The sensory communication process involves:

1. **Sensory Capture-** Special devices are used to detect touch sensations during the interaction between the patient and the end effector. The arrangement of sensors on the interaction surface influences the spatial resolution, which is the detail level of the captured touch data. In this report, "spatial resolution" refers to the count of sensors per unit area on the interaction surface (i.e. the area of contact between the end effector and the patient).
2. **Data processing and encoding-** Following the capture phase, the gathered data undergoes processing wherein it is translated into a digital format via a suitable encoding scheme. This step is crucial as it ensures that the tactile information is represented accurately and can be transmitted without loss of fidelity.
3. **Data transmission-** The encoded data is transmitted via a suitable wired or wireless mode. Distance between the end effector and remote manipulator determines the type of wired and wireless communication technology used and the protocols involved determine the encoding.
4. **Data reception and rendering-** At the remote manipulator's end, the transmitted data is captured and then rendered through compatible haptic devices. These devices are designed to intuitively convey the physical sensations, allowing the recipient to perceive the touch attributes as if they were experiencing them firsthand.

In this report, the preliminary design of a modular wearable pressure sensor array for monitoring a human end effector's palm contact forces on the patient has been discussed. This is the first prototype for achieving the sensor capture, data processing and encoding and data transmission of the tactile modality communication process.

Contributions of this report are:

(1) Specifying a reproducible design method of the modular wearable pressure sensor array.

(2) Suggesting a closed loop two-way communication system where the produced design and its future iterations can be implemented.

III. Design Specifications

The overall purpose of this design is to provide the end effector with a modular wearable device that enables the remote manipulator to monitor the contact force during physical interventions. Original motivation behind the development of this design is to facilitate remote delivery of cardiopulmonary resuscitation during emergency situations when transporting the patient might be difficult and involve high latency.

The primary functions of the design include:

(1) Capturing contact force values from different points on the end effector's palm.
(2) Encoding and wireless transmission of the captured contact force values.

The objectives of the design are:

(1) To be able to be embeddable on a wearable such as gloves,
(2) To be modular and reconfigurable with respect to the spatial distribution of the pressure sensing units.

III. Design Methodology

The design methodology involved selecting the sensors for reading applied force values and building the control circuit consisting of a buffer, microcontroller, multiplexer and a wireless communication module. Component selection process and their configuration has been detailed. The build process and testing phase has been described in the "Experiments and Tests" section.

A. Pressure Sensor Elements

In order to capture the contact pressure of the end effector's palm on the patient, several sensors were considered and a selection process was employed. The selection process primarily focused on compatibility of the pressure sensors with a fabric while achieving the primary function 1 (i.e. flexibility of the sensor, lightweightness, force sensitivity, and less number of components for data acquisition). A force sensitive resistor (FSR) was chosen for the purpose. This device changes its resistance as pressure is applied to it, The characteristic curve (Fig.1) of the device is provided in the datasheet form the manufacturer (Interlink Devices) [3]. To deduce the force the end effector applies on the patient, the real time resistance of the FSR needs to be determined through a voltage divider circuit. The equation for determining the real-time resistance of the FSR (Rvar) is as follows:

$$R_{var} = V_{in} / (V_{cc} / (R_{var} + R_f))$$

where, V_{in} is the voltage at the node joining the FSR to the known resistor of resistance value (R_f). V_{cc} is the input voltage of the voltage divider. The FSR's other node was connected to the GND node, hence V_{in} (according to Kirchoff's voltage law) becomes:

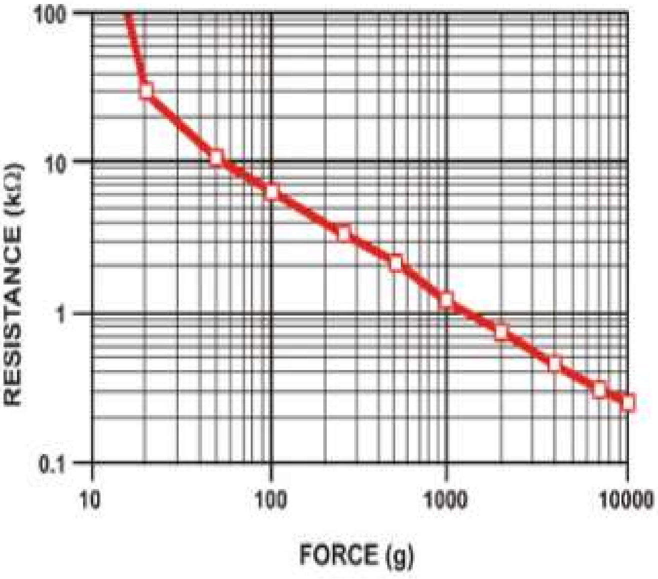

Fig. 1. Instantaneous resistance versus applied force curve of the 402 FSR.

$$V_{in} = (V_{cc} / (R_{var} + R_f)) \cdot R_{var}$$

Hence, by reading the V_{in} values using a suitable microcontroller the real time applied contact force can be deduced. Theoretical characteristic curve of V_{in} for R_{var} values in the range of 1 to 10 kOhm was plotted (Fig.2) to select a suitable R_f.

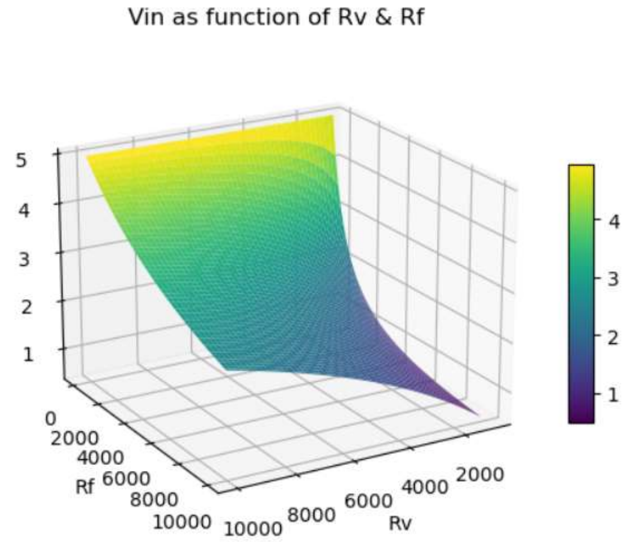

Fig. 2. Vin as a function of the two resistances in the voltage divider circuit.

Based on the graph in Fig.2 and to keep the total current drawn in the voltage divider circuit to be under 100 mA, the R_f chosen was 11MOhm. Fig.3. shows the schematic view of the voltage divider circuit.

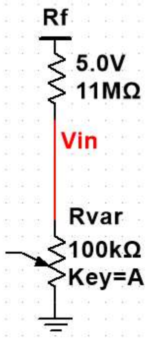

Fig. 3. Voltage divider circuit for calculating realtime resistance of the FSR and hence deducing the applied contact force.

B. Buffer circuit for Vin

To ensure that the microcontroller can accurately read the Vin values without drawing substantial current from the voltage divider circuit, which could potentially alter the measured voltage, an input buffer stage was introduced before the Vin reaches the microcontroller. This buffering step serves to isolate the microcontroller from the circuit, thus maintaining the integrity of the voltage signal and preventing any undesirable loading effects. The operational amplifier used for building the unity-gain buffer (buffer that does not amplify the V_{in}) is MCP6004 hence it showed ideal OpAmp behavior. The schematic diagram with the voltage divider circuit and the OpAmp buffer is shown in Fig. 4.

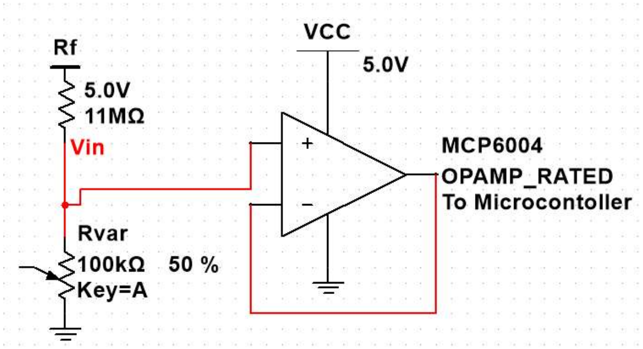

Fig. 4. Voltage divider circuit connected to the OpAmp buffer prestage to the input into the microcontroller .

C. Microcontroller selection

The selection criteria for the microcontroller is small in size for wearable application while having sufficient number of GPIO (General Purpose Input Output) pins for reading the values from the FSRs and transmitting the data. XIAO RP2040 microcontroller from Seeed Studio [5] was the perfect fit for this application. It had Type-C USB input for power and sufficient number of the GPIO pins to poll the array of FSRs sequentially (with a fast 133 MHz clock) via an analog multiplexer (since the V_{in} signal is an analog signal) [6].

D. Wireless communication module

Radio frequency communication for up to a range of 1000 Meters was facilitated by the HC-12 long-range wireless module. Communication between the HC-12 and the XIAO RP2040 was taken care of by an AT command library [4].

IV. EXPERIMENTS AND RESULTS

After selecting the components and developing the preliminary design, the circuit was built and installed in gloves and some evaluation tests were run. The step by step build process and test results are given in this section.

A. Experiment 1: Testing the buffer circuit

To ensure the unity gain buffer worked correctly, the following experimental procedure was used:

(1) Configure the unity gain buffer without the FSR once and with the FSR as shown in Fig. 4 and Fig. 5.
(2) For the setup without the FSR, feed in a test input signal (squarewave of 5 Hz) into the buffer using a signal generator.
(3) Power the quad OpAmp (MCP6004) using a 5V DC power supply with a current limitation of 100 mA.
(4) Probe the buffer output with a digital oscilloscope and observe output waveform.
(5) Touch/apply pressure to the FSR units and observe the changes in the waveform of the oscilloscope.

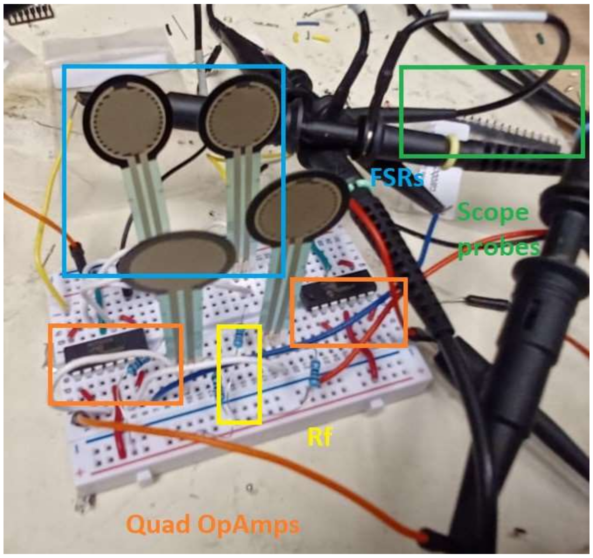

Fig. 5. Experimental setup for testing the unity gain buffer

The test results obtained in the process are given below. They demonstrate the expected behavior closer to the predictions of the graph in Fig. 2.

Fig. 6. shows the behavior of the buffer on the square wave input, The buffered signal is seen without significant distortion,

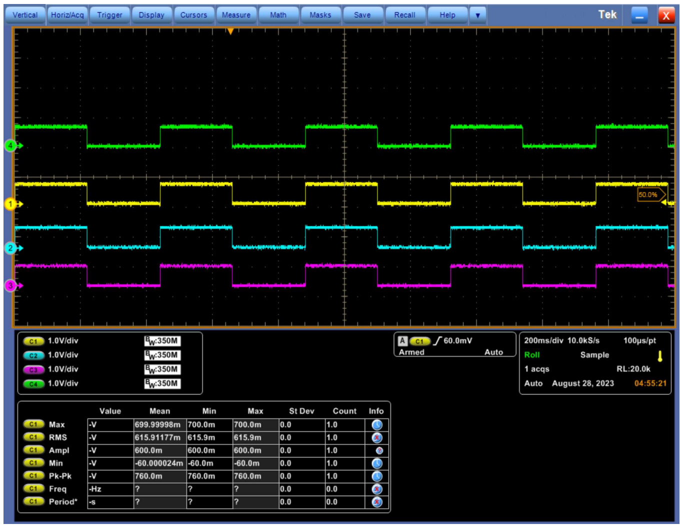

C1 1.0V/div BW:350M
C2 1.0V/div BW:350M
C3 1.0V/div BW:350M
C4 1.0V/div BW:350M

A C1 60.0mV
Armed Auto

200ms/div 10.0kS/s 100µs/pt
Roll Sample
1 acqs RL:20.0k
Auto August 28, 2023 04:55:21

	Value	Mean	Min	Max	St Dev	Count
C1 Max	-V	699.99998m	700.0m	700.0m	0.0	1.0
C1 RMS	-V	615.91177m	615.9m	615.9m	0.0	1.0
C1 Ampl	-V	600.0m	600.0m	600.0m	0.0	1.0
C1 Min	-V	-60.000024m	-60.0m	-60.0m	0.0	1.0
C1 Pk-Pk	-V	760.0m	760.0m	760.0m	0.0	1.0
C1 Freq	-Hz	?	?	?	0.0	0.0
C1 Period*	-s	?	?	?	0.0	0.0

Fig. 6. Oscilloscope reading of the buffer output and original signal input (blue:original input signal, other colors: buffered output).

C1 2.0V/div BW:350M
C2 2.0V/div BW:350M
C3 2.0V/div BW:350M
C4 2.0V/div BW:350M

A C1 40.0mV
Armed Auto

200ms/div 10.0kS/s 100µs/pt
Roll Sample
1 acqs RL:20.0k
Auto August 28, 2023 07:04:39

	Value	Mean	Min	Max	St Dev	Count
C1 Max	-V	5.12	5.12	5.12	0.0	1.0
C1 RMS	-V	5.0397376	5.04	5.04	0.0	1.0
C1 Ampl	-V	0.0	0.0	0.0	0.0	1.0
C1 Min	-V	4.96	4.96	4.96	0.0	1.0
C1 Pk-Pk	-V	160.0m	160.0m	160.0m	0.0	1.0
C1 Freq	-Hz	?	?	?	0.0	0.0
C1 Period*	-s	?	?	?	0.0	0.0

C1 2.0V/div BW:350M
C2 2.0V/div BW:350M
C3 2.0V/div BW:350M
C4 2.0V/div BW:350M

A C1 40.0mV
Armed Auto

200ms/div 10.0kS/s 100µs/pt
Roll Sample
1 acqs RL:20.0k
Auto August 28, 2023 07:05:11

	Value	Mean	Min	Max	St Dev	Count
C1 Max	-V	5.12	5.12	5.12	0.0	1.0
C1 RMS	-V	5.0397376	5.04	5.04	0.0	1.0
C1 Ampl	-V	0.0	0.0	0.0	0.0	1.0
C1 Min	-V	4.96	4.96	4.96	0.0	1.0
C1 Pk-Pk	-V	160.0m	160.0m	160.0m	0.0	1.0
C1 Freq	-Hz	?	?	?	0.0	0.0
C1 Period*	-s	?	?	?	0.0	0.0

C1 2.0V/div BW:350M
C2 2.0V/div BW:350M
C3 2.0V/div BW:350M
C4 2.0V/div BW:350M

A C1 40.0mV
Armed Auto

200ms/div 10.0kS/s 100µs/pt
Roll Sample
1 acqs RL:20.0k
Auto August 28, 2023 07:04:29

	Value	Mean	Min	Max	St Dev	Count
C1 Max	-V	5.12	5.12	5.12	0.0	1.0
C1 RMS	-V	5.0397376	5.04	5.04	0.0	1.0
C1 Ampl	-V	0.0	0.0	0.0	0.0	1.0
C1 Min	-V	4.96	4.96	4.96	0.0	1.0
C1 Pk-Pk	-V	160.0m	160.0m	160.0m	0.0	1.0
C1 Freq	-Hz	?	?	?	0.0	0.0
C1 Period*	-s	?	?	?	0.0	0.0

C1 2.0V/div BW:350M
C2 2.0V/div BW:350M
C3 2.0V/div BW:350M
C4 2.0V/div BW:350M

A C1 40.0mV
Armed Auto

200ms/div 10.0kS/s 100µs/pt
Roll Sample
1 acqs RL:20.0k
Auto August 28, 2023 07:00:00

	Value	Mean	Min	Max	St Dev	Count
C1 Max	-V	5.12	5.12	5.12	0.0	1.0
C1 RMS	-V	5.0397376	5.04	5.04	0.0	1.0
C1 Ampl	-V	0.0	0.0	0.0	0.0	1.0
C1 Min	-V	4.96	4.96	4.96	0.0	1.0
C1 Pk-Pk	-V	160.0m	160.0m	160.0m	0.0	1.0
C1 Freq	-Hz	?	?	?	0.0	0.0
C1 Period*	-s	?	?	?	0.0	0.0

Fig. 7. Oscilloscope readings of the FSR response to touch stimulus from the human hand.

Fig.7. shows the set of images involving the tests run by applying pressure to the FSRs. The first graphs show the V_{in} behavior of a single FSR with periodic stimulus applied to it. Similarly, the last graph of the same figure demonstrates the stimulation of the 4 FSRs all at the same time.

B. *Experiment 2: Building & testing the control circuit*

The control circuit consists of the 8 of the FSR units, 8 unity gain buffers, HC-12 wireless transmission module, XIAO RP2040 Microcontroller, and a 74HC4051 16:1 multiplexer. The connections were made as per the schematic shown in Fig.8.

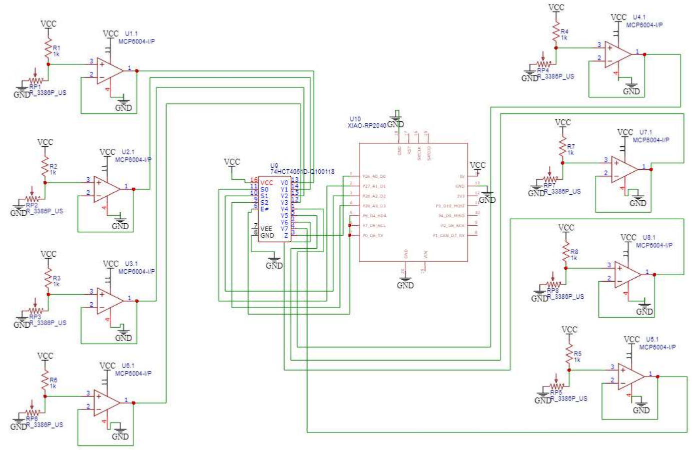

Fig. 8. Circuit diagram of the wearable device showing buffers, multiplexer and the microcontroller. HC-12's footprint was not available in the EDA software hence not shown.

The system was built incrementally in modules. All of the circuit components were soldered onto a perfboard, continuity tests were run using a digital multimeter and the final circuit was tested.

The modules (shown in Fig. 10) developed were as follows:

(1) Module 1: Each of the FSR units are attached to the voltage-divider circuit through a power plug and can be detached or attached or reconfigured as required.
(2) Module 2: Control circuit for the FSR consisting of the multiplexer for sequentially polling the FSRs to find out the force applied at each point.

The modules developed can be all detached and reattached via flexible cables (hence, the modularity). The test procedure was as follows:

(1) Apply pressure to the FSRs through human hand and capture the raw analog force signals.
(2) Power the circuit through a power bank and see if the circuit transmits the pressure data to another off the shelf receiving unit and log the received data
(3) Check for errors in the functionality of the device and iterate again if needed

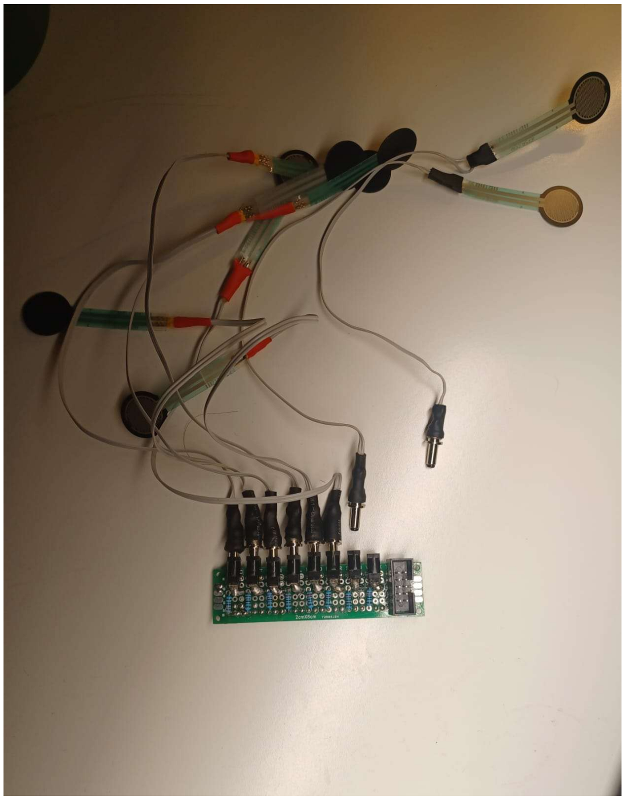

Fig. 9. Module 1 with the FSRs soldered to the power plug that are detachable or attachable to the voltage divider circuit.

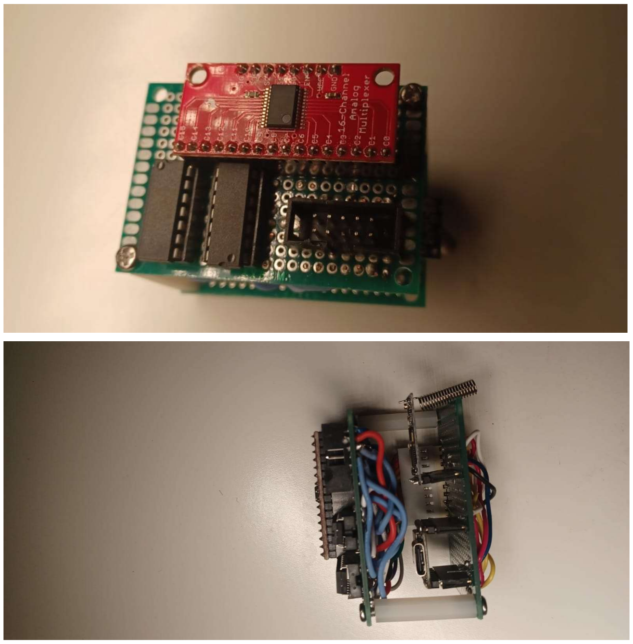

Fig. 10. Module 2 Top and side view of the control circuit consisting of the multiplexer, microcontroller, and the wireless transmission module.

Spatial distribution scheme of the FSRs on the palm side of the gloves is given in Fig. 11. The scheme is reconfigurable in terms of removing or adding more FSRs, although with an upper limit of 8 FSRs per voltage divider module

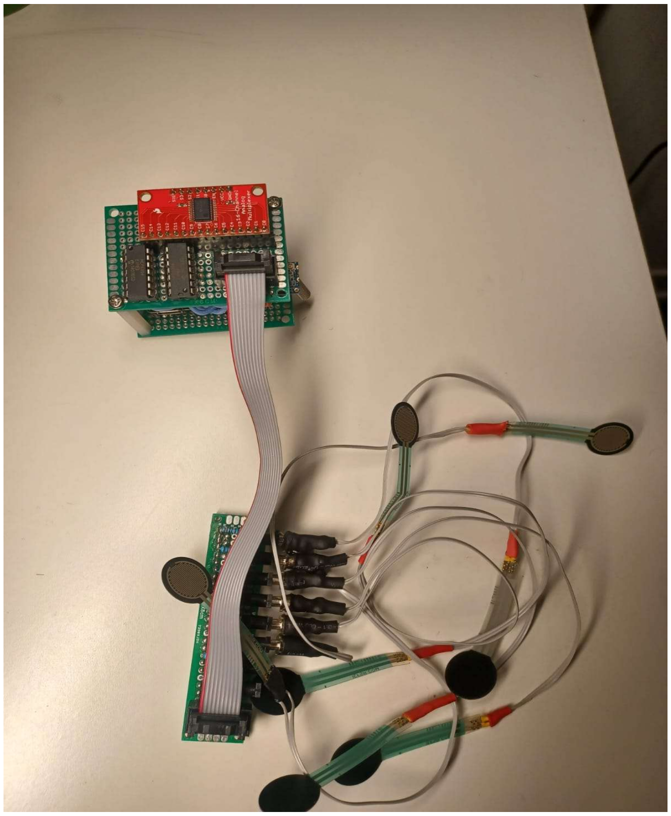

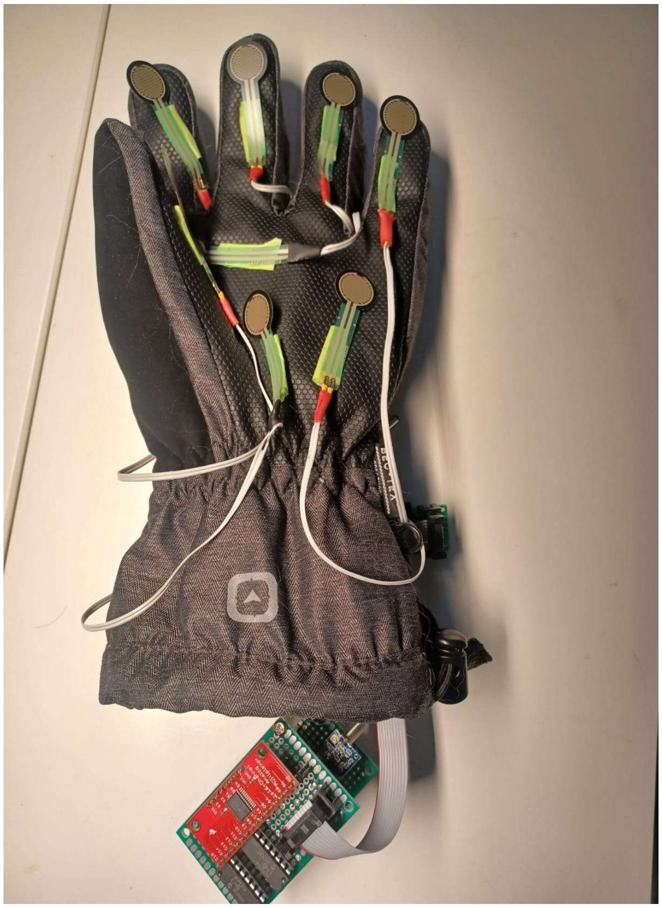

.

Fig .11.Top: fully connected module 1 and module 2; the connection is made via a flexible ribbon connector; bottom: the system embedded in a gloves for human end effector usage.

The test results obtained from the receiver's side (what would be the remote manipulator's side when the prototype is

implemented in a real world setting) are plotted (Fig. 13). Each of the plots correspond to a single force sensing unit on the gloves. There were 8 of these captures, however, only 4 are provided to avoid redundancy. As seen, different points of the palm of the end effector apply varying forces. There is a spatial and temporal variability to this process.

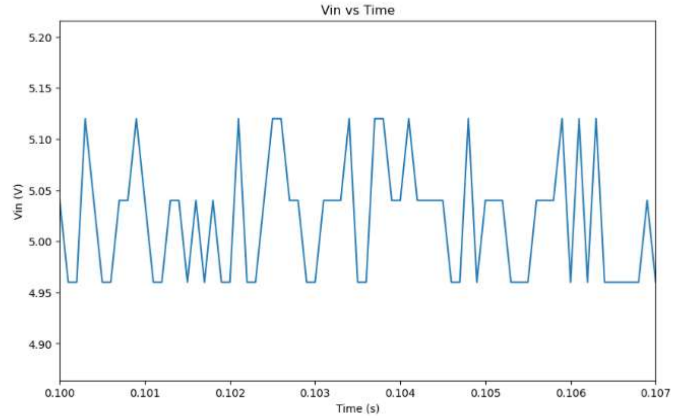

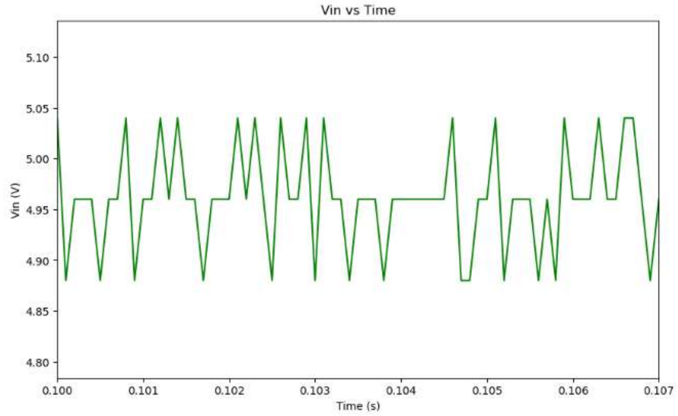

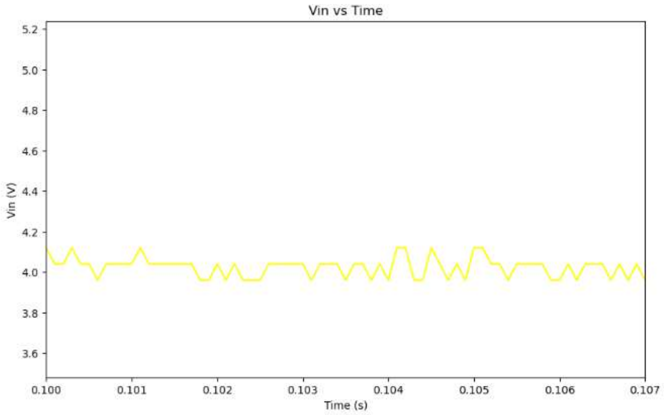

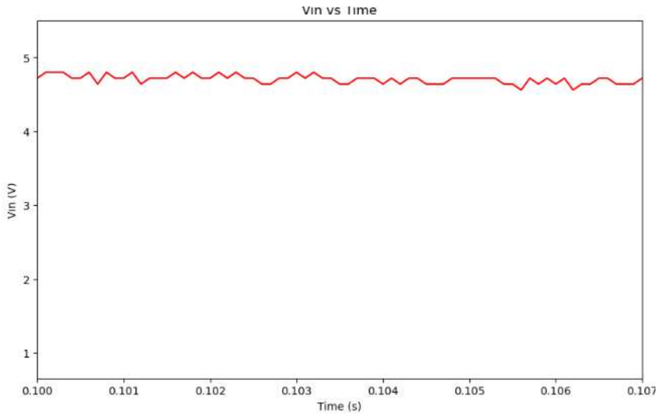

Fig. 13. Waveform plots of the received data from the assembled piece (module 1 and module 2 embedded on a glove and force applied on a wooden table). Each waveform corresponds to one FSR (one spot in the palm of the end effector that is applying force).

V. CONCLUSION AND DISCUSSION

This report presented a preliminary design of a modular force sensing system that captured the end effector's applied force and transmitted it to a receiver (potential remote manipulator).

The results demonstrate a potential and scope for further development of the design which includes improvising the fidelity of circuit by fabricating a Printed Circuit Board, using flexible connectors, implementing faster encoding and polling algorithms and building the haptic rendering glove for the remote manipulator. Overall, there is a potential for this device to be used in remote CPR, palpation as well as physiotherapy applications where the tactile modality is crucial for diagnosis and treatment.

VI. REFERENCES

[1] Tavakoli, M., Carriere, J., & Torabi, A. (2020a). Robotics, Smart Wearable Technologies, and autonomous intelligent systems for Healthcare during the COVID-19 pandemic: An analysis of the state of the art and future vision. Advanced Intelligent Systems, 2(7), 2000071. https://doi.org/10.1002/aisy.202000071

[2] L. Massari et al., "Neuromorphic haptic glove and platform with gestural control for tactile sensory feedback in medical telepresence applications," *2018 IEEE International Symposium on Medical Measurements and Applications (MeMeA),* Rome, Italy, 2018, pp. 1-6, doi: 10.1109/MeMeA.2018.8438597.

[3] Sparkfun. (2010, October 26). Description - Sparkfun Electronics. FSR 402 Data Sheet.

[4] smart-prototyping. (2016, December 2). HC-12 user manual V2.4 161202 - smart prototyping. HC-12 WIRELESS RF UART COMMUNICATION MODULE V2.4 USER MANUAL.

[5] Seeed Studio. (2023, January 11). Getting started: Seeed studio wiki. Seeed Studio Wiki RSS. https://wiki.seeedstudio.com/XIAO-RP2040/

[5] Seeed Studio. (2023, January 11). Getting started: Seeed studio wiki. Seeed Studio Wiki RSS. https://wiki.seeedstudio.com/XIAO-RP2040/

[6]Creatron Inc. (2022, November 19). 74HC4067 8 ch multiplexer breakout. Creatron Inc. https://www.creatroninc.com/product/74hc4067-8-channel-multiplexer-breakout/